

Differences in Carbon Isotope Discrimination of Three Variants of D-Ribulose-1,5-bisphosphate Carboxylase/Oxygenase Reflect Differences in Their Catalytic Mechanisms*[§]

Received for publication, July 30, 2007, and in revised form, October 3, 2007. Published, JBC Papers in Press, October 9, 2007, DOI 10.1074/jbc.M706274200

Dennis B. McNevin^{‡§}, Murray R. Badger[‡], Spencer M. Whitney[‡], Susanne von Caemmerer[‡],
 Guillaume G. B. Tcherkez[¶], and Graham D. Farquhar^{¶1}

From [‡]Molecular Plant Physiology and [¶]Environmental Biology, Research School of Biological Sciences, The Australian National University, Canberra, and the [§]School of Health Sciences, University of Canberra, Bruce, Australian Capital Territory 2601, Australia and the [¶]Laboratoire d'Ecophysiologie Végétale, Université Paris Sud XI, 91405 Orsay Cedex, France

The carboxylation kinetic (stable carbon) isotope effect was measured for purified D-ribulose-1,5-bisphosphate carboxylases/oxygenases (Rubiscos) with aqueous CO₂ as substrate by monitoring Rayleigh fractionation using membrane inlet mass spectrometry. This resulted in discriminations (Δ) of 27.4 ± 0.9‰ for wild-type tobacco Rubisco, 22.2 ± 2.1‰ for *Rhodospirillum rubrum* Rubisco, and 11.2 ± 1.6‰ for a large subunit mutant of tobacco Rubisco in which Leu³³⁵ is mutated to valine (L335V). These Δ values are consistent with the photosynthetic discrimination determined for wild-type tobacco and transplasmic tobacco lines that exclusively produce *R. rubrum* or L335V Rubisco. The Δ values are indicative of the potential evolutionary variability of Δ values for a range of Rubiscos from different species: Form I Rubisco from higher plants; prokaryotic Rubiscos, including Form II; and the L335V mutant. We explore the implications of these Δ values for the Rubisco catalytic mechanism and suggest that Rubiscos that are associated with a lower Δ value have a less product-like carboxylation transition state and/or allow a decarboxylation step that evolution has excluded in higher plants.

Measurement of the enzymatic depletion of the stable carbon isotope ¹³C with respect to the relatively abundant ¹²C is a valuable technique for understanding kinetic reaction mechanisms. Plant enzymes that have been analyzed in this way include carbonic anhydrase (1), phosphoenolpyruvate carboxylase (EC 4.1.1.31) (2–4), and D-ribulose-1,5-bisphosphate carboxylase/oxygenase (Rubisco²; EC 4.1.1.39) (5–7). Models of carbon isotope discrimination in C₃ plants (8, 9), C₄ plants (10), C₃-C₄ intermediates (11), and, more recently, Crassulacean

acid metabolism plants (12–14) also form the basis for explaining ¹³C depletion in plant material. This depletion is expressed in terms of the carbon isotope ratio (R) of a substance defined as in Equation 1 (15, 16).

$$R = \frac{[^{13}\text{C}]}{[^{12}\text{C}]} \quad (\text{Eq. 1})$$

The isotope composition of a substance, $\delta^{13}\text{C}$ or δ , is given by Equation 2 (17, 18),

$$\delta^{13}\text{C} = \delta = \frac{R}{R_{\text{std}}} - 1 \quad (\text{Eq. 2})$$

where R_{std} is the isotope ratio for a given standard (marine limestone from the Pee Dee Cretaceous belemnite formation in South Carolina or an artificial version from Vienna (referred to as VPDB)). The units for δ are usually expressed in terms of parts/thousand or “parts/mil” (‰). For a process that transforms a substrate or source from one isotope composition (R_S) to a product with composition R_P , the isotope effect or fractionation factor (α) is as in Equation 3 (19).

$$\alpha = \frac{[^{13}\text{C}_S]/[^{12}\text{C}_S]}{[^{13}\text{C}_P]/[^{12}\text{C}_P]} = \frac{R_S}{R_P} = \frac{R_S/R_{\text{std}}}{R_P/R_{\text{std}}} = \frac{1 + \delta_S}{1 + \delta_P} \quad (\text{Eq. 3})$$

The isotope fractionation or discrimination (Δ) associated with this process is then as in Equation 4 (15).

$$\Delta = \alpha - 1 = \frac{1 + \delta_S}{1 + \delta_P} - 1 = \frac{\delta_S - \delta_P}{1 + \delta_P} \approx \delta_S - \delta_P \quad (\text{Eq. 4})$$

A kinetic isotope effect occurs when a substrate or source is continuously converted into a product with fractionation against the heavier isotope. For Rubisco, where ¹²C and ¹³C are competing for the same active site, the isotope effect associated with CO₂ fixation can be shown to be as in Equation 5 (8, 20),

$$\alpha_{\text{enzyme}} = \frac{k_{\text{cat}}^{12}/K_M^{12}}{k_{\text{cat}}^{13}/K_M^{13}} \quad (\text{Eq. 5})$$

where k_{cat}^{12} and k_{cat}^{13} are the turnover numbers for ¹²C and ¹³C, respectively, and K_M^{12} and K_M^{13} are the apparent Michaelis-Menten (half-saturation) constants for ¹²C and ¹³C, respectively. In this case, enrichment and discrimination are independent of the concentration of either isotope, a fact supported by

* The costs of publication of this article were defrayed in part by the payment of page charges. This article must therefore be hereby marked “advertisement” in accordance with 18 U.S.C. Section 1734 solely to indicate this fact.

† This article was selected as a Paper of the Week.

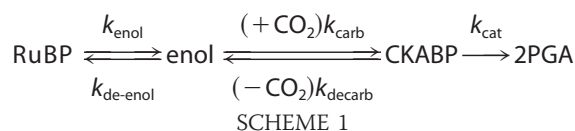
§ The on-line version of this article (available at <http://www.jbc.org>) contains a supplemental “Appendix.”

¹ To whom correspondence should be addressed: Environmental Biology, Research School of Biological Sciences, The Australian National University, G.P.O. Box 475, Canberra, ACT 2601, Australia. Tel.: 61-2-6125-3743; Fax: 61-2-6125-4919; E-mail: graham.farquhar@anu.edu.au.

² The abbreviations used are: Rubisco, D-ribulose-1,5-bisphosphate carboxylase/oxygenase; RuBP, D-ribulose 1,5-bisphosphate; CKABP, 2-carboxy-3-keto-D-arabinitol 1,5-bisphosphate; WT, wild-type; EPPS, 4-(2-hydroxyethyl)-1-piperazinepropanesulfonic acid.

Christeller *et al.* (5), who found no effect on the discrimination of soybean Rubisco by bicarbonate concentrations in the 2.5–50 mM range. The discriminations of Rubiscos from a number of different species with aqueous CO₂ as substrate derived from a review of the literature are shown in Table 1.

Measurements of the kinetic isotope effect can be used to infer reaction mechanisms. Consider the carbon fixation reaction, catalyzed by Rubisco, where D-ribulose 1,5-bisphosphate (RuBP) is first enolized and then combines with CO₂ to form 3-phosphoglycerate according to Scheme 1 (21–23).



Here, enol refers to enolized RuBP, and 2-carboxy-3-keto-D-arabinitol 1,5-bisphosphate (CKABP) is the carboxylated reaction intermediate in this simplified scheme (24), whether the latter exists in this form or as the hydrated *gem*-diol (25). CKABP will undergo subsequent hydrolysis and cleavage to form two molecules of 3-phosphoglycerate, whereas the *gem*-diol will require only cleavage. The intrinsic reaction steps are characterized by the rate constants (forwards and backwards) for enolization (k_{enol} and $k_{\text{de-enol}}$) and for carboxylation (k_{carb} and k_{decarb}) and the turnover number (k_{cat} , which may be two steps combined). Because it is only the steps involving the carbon atom from CO₂ that have an effect on discrimination, enolization (occurring before CO₂ addition) does not have impact on fractionation by the enzyme (see supplemental “Appendix”). Similarly, the turnover number does not affect fractionation because neither hydration nor cleavage exhibits isotopic carbon bond formation or breakage involving the carbon atom inherited from CO₂. Then, the fractionation factor associated with CO₂ addition is as in Equation 6 (20, 26).

$$\alpha_{\text{Rubisco}} \approx \frac{k_{\text{carb}}^{12}}{k_{\text{carb}}^{13}} \cdot \frac{1 + k_{\text{decarb}}^{13}/k_{\text{cat}}}{1 + k_{\text{decarb}}^{12}/k_{\text{cat}}} \quad (\text{Eq. 6})$$

Furthermore, if the decarboxylation rate constant is very small compared with the turnover number (*i.e.* if $k_{\text{decarb}} \ll k_{\text{cat}}$), then the kinetic isotope effect for the overall enzyme-catalyzed process reduces to the kinetic isotope effect for the carboxylation step as in Equation 7.

$$\alpha_{\text{Rubisco}} \approx \frac{k_{\text{carb}}^{12}}{k_{\text{carb}}^{13}} \quad (\text{Eq. 7})$$

This is the intrinsic (carbon bond-forming) isotope effect and represents the upper limit for the total kinetic isotope effect for carboxylation catalyzed by Rubisco (1, 20). The intrinsic isotope effect will depend on the vibrational energies associated with carboxyl bond formation between isotopic carbon dioxide and enolized RuBP, and its magnitude may be estimated by the methods of Bigeleisen (27) and Melander (28). On the basis of these methods, Tcherkez *et al.* (29) predicted that the intrinsic isotope effect will increase as the carboxylation transition state comes to resemble the product, *i.e.* as it is delayed along the reaction coordinate.

We then have two possible mechanisms by which the kinetic isotope effect may differ between Rubiscos. First, the intrinsic isotope effect ($k_{\text{carb}}^{12}/k_{\text{carb}}^{13}$) may vary according to the carboxylation transition state structure with a more product-like transition state having a higher fractionation factor. Alternatively, the fractionation factor will be reduced as the decarboxylation rate increases or as the commitment of the carboxylated intermediate (CKABP) to hydrolysis and cleavage is reduced. This has the effect of replenishing free ¹²CO₂ that has been depleted by carboxylation.

Rubisco occurs as a so-called Form I enzyme in higher plants, cyanobacteria, and proteobacteria (comprising a hexadecamer of eight large and eight small subunits) and as a simpler Form II enzyme (comprising one or more dimers of large subunits) in proteobacteria and some dinoflagellates (23, 30, 31). In this study, we compare the kinetic isotope effects (in terms of discrimination (Δ)) for Rubisco from a higher plant (tobacco, Form I) and from α -proteobacterium (*Rhodospirillum rubrum*, Form II) and a large subunit mutant of tobacco Rubisco in which Leu³³⁵ is mutated to valine (L335V) (32). Leu³³⁵ sits on loop 6 of the α/β -barrel at the carboxyl-terminal end of the Rubisco large subunit (32). This loop closes over the substrate RuBP as it is bound (31, 33, 34). We speculate that this residue is involved in stabilization of the transition state for either the hydrolysis or cleavage step (or both).

We have measured Δ , based on Rayleigh fractionation, by continuous real-time measurement of individual carbon isotope concentrations via membrane inlet mass spectrometry (35). We show that the Δ values for *R. rubrum* and L335V tobacco Rubiscos are consistent with photosynthetic discrimination by transgenic tobacco plants in which native Rubisco has been replaced with Form II or a mutant variant. We examine the implications of the differences in Δ values for the catalytic mechanism of the variant enzymes.

EXPERIMENTAL PROCEDURES

Wild-type and Transgenic Tobacco Plants—Tobacco (*Nicotiana tabacum*) grown for Rubisco harvesting and leaf tissue carbon isotope measurements included wild-type (WT) plants and two transplastomic mutants: one producing mutant tobacco Rubisco containing the large subunit mutation L335V (32) and one producing *R. rubrum* Rubisco (referred to as tobacco-*rubrum*) (36). As the mutants are unable to grow in air, all plants were germinated from seed in 5-liter pots of soil in a growth chamber equilibrated with air supplemented with 1% (v/v) CO₂. The air temperature was 25 °C with a 14-h photoperiod (400 $\mu\text{mol quanta m}^{-2} \text{s}^{-1}$) and 60% relative humidity. The WT plants were also grown in air in an air-conditioned glasshouse as a control.

RuBP, 2-Carboxyphenitol 1,5-Bisphosphate, and Rubisco Purification—Pure RuBP was prepared according to Kane *et al.* (37). WT Rubisco was purified from tobacco leaves by polyethylene glycol precipitation followed by crystallization via dialysis as described by Servaites (38). L335V tobacco Rubisco was purified by polyethylene glycol precipitation followed by anion-exchange chromatography (AKTA™ Explorer, Amersham Biosciences AB, Uppsala, Sweden) on a Waters Protein-Pak™ Q

Kinetic Isotope Effect for Three Rubiscos

column as described by Edmondson *et al.* (39) but omitting the final gel filtration step. *R. rubrum* Rubisco production in XL1-Blue cells transformed with plasmid pRR1 (40) was induced with 1 mM isopropyl β -D-thiogalactopyranoside at 37 °C for 6 h, and the enzyme was purified according to Andrews and Kane (41). All enzymes were >95% pure as determined by SDS-PAGE. They were snap-frozen in liquid nitrogen and stored at -80 °C in storage buffer (25 mM EPPS-NaOH, pH 8.0, 50 mM NaCl, 1 mM EDTA, and 20% (v/v) glycerol). The active-site concentration for each enzyme was determined by the 2-[¹⁴C]carboxy-D-arabinitol 1,5-bisphosphate binding method of Butz and Sharkey (42) as modified by Ruuska *et al.* (43) using 2-[¹⁴C]carboxypentitol 1,5-bisphosphate (an isomeric mixture of 2-[¹⁴C]carboxy-D-arabinitol 1,5-bisphosphate and 2-[¹⁴C]carboxyribitol 1,5-bisphosphate) that was synthesized according to Pierce *et al.* (44).

Mass Spectrometry Isotope Discrimination Analyses—CO₂ uptake in the carboxylation reactions facilitated by purified Rubiscos was monitored by membrane inlet mass spectrometry as described (35). The signals for each isotope were corrected for their zero offsets, and the corrected signals were then used to obtain a raw discrimination (Δ_{total}) with respect to aqueous CO₂ according to Equation 8,

$$1 + \Delta_{\text{total}} = \alpha_{\text{total}} = \frac{d(\ln[^{12}\text{C}])}{d(\ln[^{13}\text{C}])} \quad (\text{Eq. 8})$$

where α_{total} is the slope of a line of best fit through a plot of points ($\ln[^{13}\text{C}]$ and $\ln[^{12}\text{C}]$). An enzyme discrimination was then calculated for each reaction according to Equation 9 (35),

$$\Delta_{\text{Rubisco}} = \frac{1 + \Delta_{\text{total}}}{1 + \Delta_{\text{part}}} - 1 \quad (\text{Eq. 9})$$

where Δ_{part} is the discrimination due to partitioning of inorganic carbon between CO₂ and HCO₃⁻ in solution given by Equation 10 (35).

$$\Delta_{\text{part}} = \frac{-\Delta_{\text{eq}}}{1 + (1 + \Delta_{\text{eq}})10^{pK_{\text{eq}} - \text{pH}} + \Delta_{\text{eq}}} \quad (\text{Eq. 10})$$

Here, Δ_{eq} is the discrimination due to the equilibrium isotope effect between CO_{2(aq)}} and HCO_{3(aq)}}⁻ (relative to CO₂) equal to -8.9‰ (45), and pK_{eq} is the equilibrium dissociation constant for CO_{2(aq)}}/HCO_{3(aq)}}⁻ equal to 6.25 at 25 °C.

Rubisco Activity—Purified Rubisco was used to measure substrate-saturated carboxylase activities at 15, 20, 25, 30, and 35 °C using a ¹⁴CO₂ fixation assay based on that of Andrews (46). Reactions (200 μ l) were prepared in 7-ml scintillation vials and were buffered with 80 mM EPPS, pH 8.0, 20 mM MgCl₂, 1 mM EDTA, and 0.1 mg/ml carbonic anhydrase (Sigma). The final concentrations of purified Rubisco and NaHCO₃ varied as follows: 0.1 mg/ml WT tobacco enzyme (1.6 μ M active sites) with 20 mM NaHCO₃, 0.05 mg/ml *R. rubrum* enzyme (0.9 μ M active sites) with 40 mM NaHCO₃, and 0.15 mg/ml L335V tobacco enzyme (2.2 μ M active sites) with 20 mM NaHCO₃. One microliter of 74 MBq/ml NaH¹⁴CO₃ was added to the reac-

tions, resulting in specific activities of 15 (WT tobacco), 7 (*R. rubrum*), and 15 (L335V tobacco) Bq/nmol. The reactions were incubated for 15 min at the different temperatures before initiating catalysis by adding RuBP to a final concentration of 1 mM. After 1 min, the reactions were quenched with 100 μ l of 25% (v/v) formic acid and heated to dryness at 80 °C. The residue was dissolved in 0.5 ml of water and then mixed with 1 ml of liquid scintillant (Ultima GoldTM XR, PerkinElmer Life Sciences), and acid-stable ¹⁴C was measured in a Searle Delta 300 scintillation counter. The turnover number (k_{cat}) was calculated by dividing the carboxylation rate by the active-site content quantified by 2-[¹⁴C]carboxy-D-arabinitol 1,5-bisphosphate binding (see above).

Isotope Composition of Tobacco Leaf Tissue and Air from the Growth Environment—The isotope composition of whole leaves from tobacco plants (three each of WT, tobacco-*rubrum*, and L335V) was determined according to Wright *et al.* (47). The third and fourth leaves of each plant were harvested after 63 days (WT; ambient air), 37 days (WT; 1% CO₂), and 51 days (L335V and *R. rubrum* mutants; 1% CO₂). The mid-vein from each leaf was removed, and the leaves were then dried at 80 °C before grinding in a ball mill (Retsch GmbH, Haan, Germany). Approximately 1 mg of each dried and ground sample was dropped into an EA1110 elemental analyzer (Fisons Instruments S.p.A., Milan, Italy) in a helium carrier and combusted in a pulse of oxygen. The oxidized products were then reduced to CO₂, N₂, and water before separation in a Porapak QS packed column (Alltech Biotechnology). The pulses of pure CO₂ then passed into an IsoChrom continuous flow stable isotope ratio mass spectrometer (Micromass UK Ltd.) in the helium carrier, and the ratios of masses 45:44 and 46:44 were determined. Calibration was performed against similarly analyzed beet sucrose internal standard ($\delta^{13}\text{C} = -24.62\text{‰}$ VPDB) and Australian National University sucrose ($\delta^{13}\text{C} = -10.45\text{‰}$ VPDB). Measurements had a Craig correction applied to compensate for contributions to mass 45 from other isotopic combinations (e.g. ¹²C¹⁷O¹⁶O rather than ¹³C¹⁶O¹⁶O).

The carbon isotope composition in the air from the two growth environments (air in the glasshouse and air plus 1% (v/v) CO₂ in the growth chamber) was also sampled at least three times into a vacuum-evacuated 1-liter stainless steel cylinder. The sampled air was drawn at low pressure (<10 millibars) into a vacuum line through a dry ice/ethanol bath (to condense water vapor) and then a liquid nitrogen trap (to condense CO₂ but not O₂). The condensed CO₂ was subjected to high vacuum (<10⁻² millibars) to evacuate the trap of all but CO₂. The liquid nitrogen bath was replaced with a dry ice/ethanol bath so that CO₂ was evaporated from the trap and recondensed in a connected glass tube immersed in liquid nitrogen. The tube was sealed under vacuum with an oxyacetylene torch. The carbon isotope ratios of these samples were then determined by analysis on a GV Instruments IsoPrime stable isotope ratio mass spectrometer fitted with a dual inlet. The glass tubes containing the sample CO₂ were broken in an evacuated tube cracker, expanding the gas into the bellows of the dual inlet. The bellows were then compressed to produce a beam of ~8 nA for beam 1 (mass 44). The reference bellows were filled with a laboratory internal standard CO₂ ($\delta^{13}\text{C} = -25.54\text{‰}$ VPDB), and the two gases

TABLE 1

Discrimination for Rubiscos from a number of different species with aqueous CO₂ as substrate and with errors as reported

The discrimination with respect to gaseous CO₂ (parameter *b*) is ~1‰ greater than the values shown here. In the first column, C₃ and C₄ refer to the photosynthetic pathways, and CCM refers to an aquatic CO₂-concentrating mechanism. The probable CO₂ and O₂ environment during Rubisco catalysis is indicated in the fourth column.

Rubisco form	Species	Common name	CO ₂ and O ₂ environment	Δ	Conditions	Source
Form 1A	<i>S. velum</i> symbiont	Bivalve clam symbiont	Low-to-medium CO ₂ , 21% O ₂	23.2–25.6 (95)	24 °C, pH 8.5	Ref. 62
Form IB, C ₄	<i>S. bicolor</i>	Sorghum	Medium CO ₂ , 21% O ₂	33.7 ± 6.6	24 °C, pH 8.2	Ref. 2
Form IB, C ₄	<i>S. bicolor</i>	Sorghum	Medium CO ₂ , 21% O ₂	18.3	37 °C, pH 8.2	Ref. 2
Form IB, C ₃	<i>G. max</i>	Soybean	Low CO ₂ , 21% O ₂	28.3 ± 1.5	15–35 °C, 2–50 mM HCO ₃ ⁻	Ref. 5
Form 1B, C ₃	<i>Gossypium</i>	Cotton	Low CO ₂ , 21% O ₂	27.1 ± 3.5	35 °C, pH 7.5	Ref. 63
Form 1B, C ₃	<i>S. oleracea</i>	Spinach	Low CO ₂ , 21% O ₂	29.7 ± 0.8	25 °C, pH 7.0	Ref. 6
Form 1B, C ₃	<i>S. oleracea</i>	Spinach	Low CO ₂ , 21% O ₂	29 ± 1	25 °C, pH 8.0	Ref. 6
Form 1B, C ₃	<i>S. oleracea</i>	Spinach	Low CO ₂ , 21% O ₂	26.4 ± 0.6	25 °C, pH 9.0	Ref. 6
Form 1B, C ₃	<i>S. oleracea</i>	Spinach	Low CO ₂ , 21% O ₂	29.0 ± 0.3	pH 7.6	Ref. 7
Form 1B, C ₃	<i>S. oleracea</i>	Spinach	Low CO ₂ , 21% O ₂	30.3 ± 0.8	pH 8.5	Ref. 7
Form 1B, C ₃	<i>S. oleracea</i>	Spinach	Low CO ₂ , 21% O ₂	26.2–29.8 (95)	24 °C, pH 8.5	Ref. 62
Form IB, CCM	<i>Anacystis nidulans</i>		High CO ₂ , 21% O ₂	22.0 ± 0.2	pH 8.1	Ref. 7
Form II	<i>R. rubrum</i>		High CO ₂ , low O ₂	17.8 ± 0.8	25 °C, pH 7.8	Ref. 50
Form II	<i>R. rubrum</i>		High CO ₂ , low O ₂	19–24	pH 7.9, 2–25 mM Mg ²⁺	Ref. 7
Form II	<i>Riftia pachyptila</i> endosymbiont		High CO ₂ , low O ₂	19.5 ± 1.0	30 °C, pH 8.0	Ref. 64

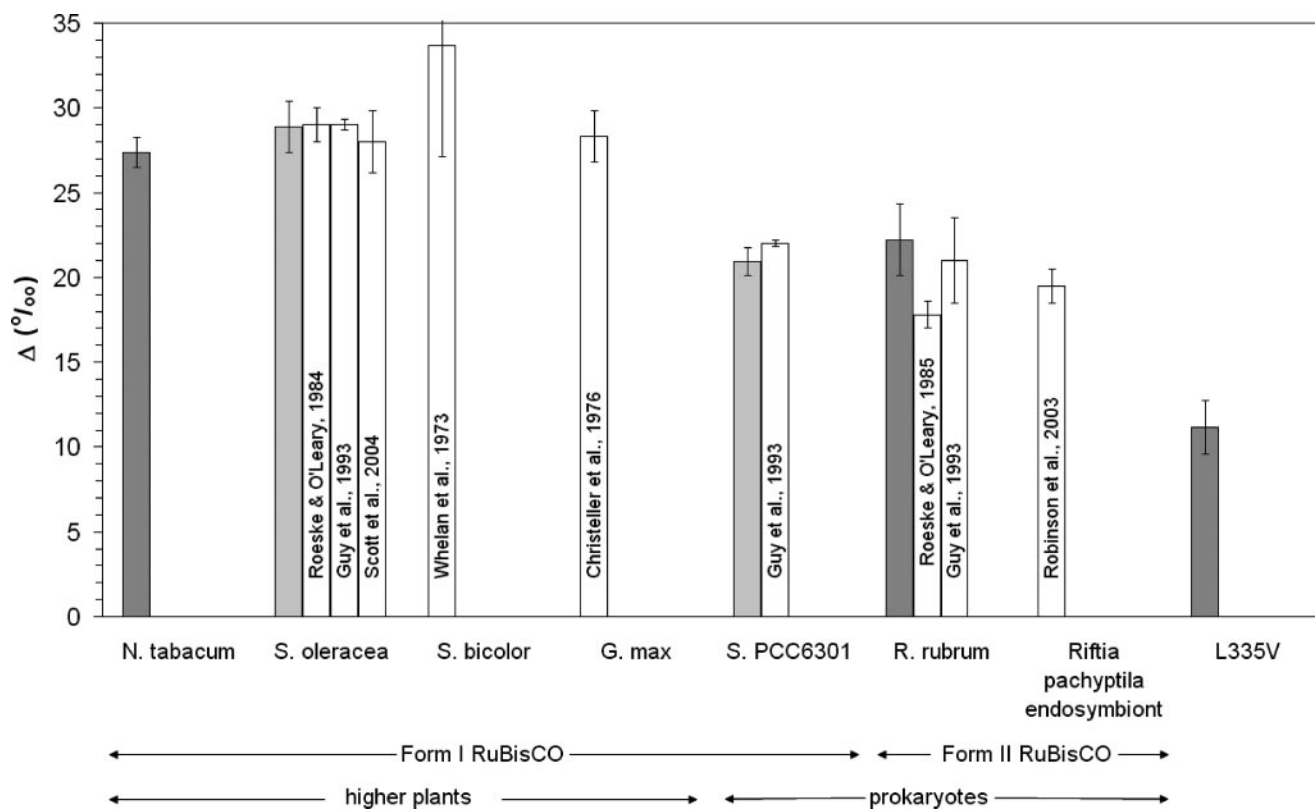


FIGURE 1. Discrimination (Δ) with respect to aqueous CO₂ for purified Rubiscos from WT tobacco ($n = 5$), *R. rubrum* ($n = 12$), and L335V tobacco ($n = 4$) measured by us in this study (dark gray bars with S.D.) together with discrimination for Rubiscos from spinach and *Synechococcus* measured by us previously (light gray bars with S.D.) (35) and discrimination for Rubiscos from other species measured by other workers (white bars with errors as reported) (Table 1). The discrimination with respect to gaseous CO₂ (parameter *b*) is ~1‰ greater than the values shown here.

were compared using six pulses of each. The overall precision of the analyses was ~0.1‰.

RESULTS

The measured enzyme discriminations (Δ) with respect to aqueous CO₂ were $27.4 \pm 0.9\text{‰}$ for WT tobacco, $22.2 \pm 2.1\text{‰}$ for *R. rubrum*, and $11.2 \pm 1.6\text{‰}$ for L335V tobacco, all expressed with respect to aqueous CO₂ as the source. These and other enzyme discriminations measured by us (35) and other workers (Table 1) are shown in Fig. 1 for discriminations

measured under comparable experimental conditions. The Rubiscos are classified as of either higher plant or prokaryotic origin and as either Form I or II.

The maximum carboxylation rate (k_{cat} (s⁻¹)) was determined for each purified enzyme at temperatures of 15, 20, 25, 30, and 35 °C. These data were used to construct an Arrhenius plot (Fig. 2) of $R \ln k_{\text{cat}}$ versus T^{-1} (K⁻¹), where the slope is the activation energy (E_a , kJ/mol), for hydrolysis/cleavage of the CKABP intermediate according to Equation 11 (see supplemental "Appendix"),

Kinetic Isotope Effect for Three Rubiscos

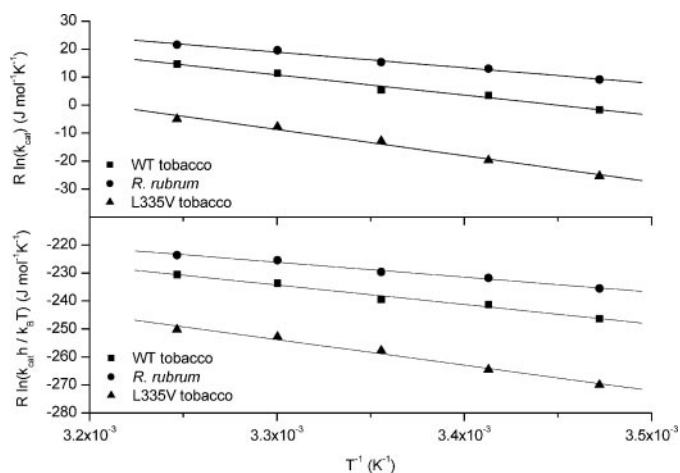


FIGURE 2. Arrhenius plots (upper panel) and free energy plots (lower panel) for purified Rubiscos from WT tobacco, *R. rubrum*, and L335V tobacco.

$$R \frac{d \ln k_{\text{cat}}}{d(T^{-1})} = -E_a \quad (\text{Eq. 11})$$

and where R is the molar gas constant. The turnover number (k_{cat}) is also related to the standard free energy difference (ΔG^\ddagger) between the intermediate and the transition state for hydrolysis/cleavage according to Equation 12 (see supplemental "Appendix"),

$$R \ln \left(\frac{k_{\text{cat}} h}{k_B T} \right) = -\frac{\Delta G^\ddagger}{T} = \Delta S^\ddagger - \frac{\Delta H^\ddagger}{T} \quad (\text{Eq. 12})$$

where h is the Planck constant; k_B is the Boltzmann constant; and ΔS^\ddagger and ΔH^\ddagger are the standard entropy and standard enthalpy differences, respectively, between the intermediate and the transition state for hydrolysis/cleavage (*i.e.* the transition state value minus the bound intermediate value). Hence, a plot of the left-hand side of this equation *versus* T^{-1} has a slope equal to $-\Delta H^\ddagger$ and an intercept (at $T^{-1} = 0$ or $T \rightarrow \infty$) equal to ΔS^\ddagger (Fig. 2). The activation energy is related to (and, for ambient temperatures, almost equal to) the standard enthalpy difference according to Equation 13 (see supplemental "Appendix").

$$E_a = \Delta H^\ddagger + RT \approx \Delta H^\ddagger \quad (\text{Eq. 13})$$

The activation energy and standard entropy and enthalpy differences obtained from Fig. 2 are shown for each of the purified enzymes in Fig. 3, together with the free energy difference at 25 °C obtained from Equation 14.

$$\Delta G^\ddagger = \Delta H^\ddagger - T\Delta S^\ddagger = \Delta H^\ddagger - (298 \text{ K})\Delta S^\ddagger \quad (\text{Eq. 14})$$

Both ΔH^\ddagger and ΔS^\ddagger depend on temperature, but in the temperature range investigated, their variation is clearly negligible, so they are considered constant. Furthermore, the entropic component of the free energy difference ($T\Delta S^\ddagger$) does not vary significantly between 15 and 35 °C, and hence, the total free energy difference (ΔG^\ddagger) is relatively constant in this temperature range.

The isotope compositions of leaf tissues (δ_{leaf}) from the tobacco plants with WT, *R. rubrum*, and L335V Rubiscos are shown in Fig. 4, together with the isotope compositions of the air in the growth

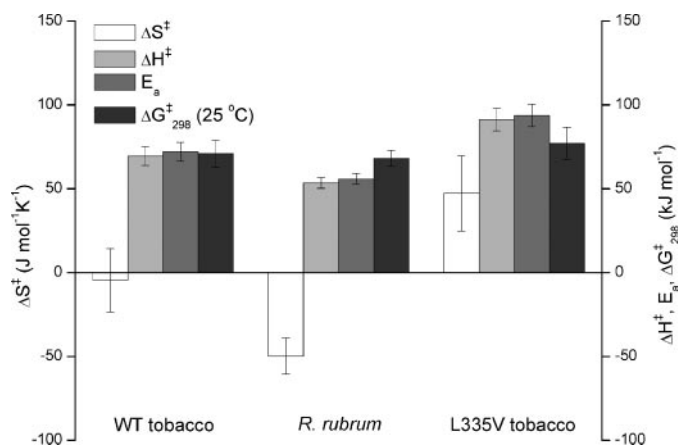


FIGURE 3. Standard entropy difference (ΔS^\ddagger ; left axis), standard enthalpy difference (ΔH^\ddagger ; right axis), and standard free energy difference at 25 °C (ΔG^\ddagger_{298} ; right axis) associated with k_{cat} as well as activation energy (E_a ; right axis) for hydrolysis/cleavage for purified Rubiscos from WT tobacco, *R. rubrum*, and L335V tobacco. Error bars represent S.E. of slopes and intercepts derived from Fig. 2.

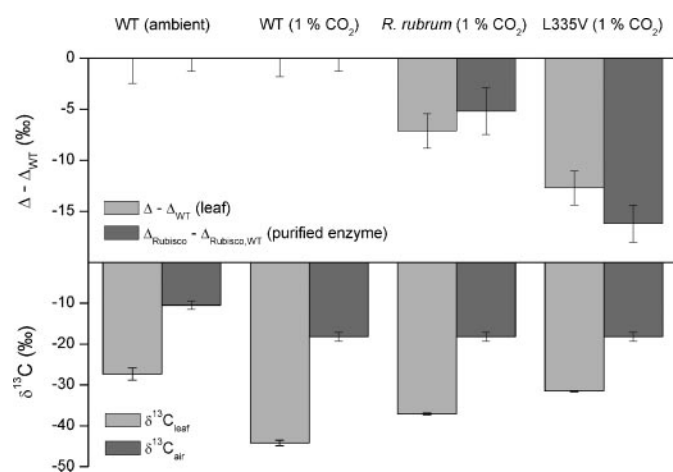


FIGURE 4. Lower panel, isotope compositions (δ_{leaf}) of leaf tissues from the tobacco plants grown in ambient air (WT) and in 1% CO_2 (WT tobacco plants, *R. rubrum* transgenic tobacco plants, and L335V mutant transgenic tobacco plants). Error bars represent S.D. ($n = 3$). For each plant, the total δ_{leaf} can be divided into the isotope composition of the air in which the plant was grown (δ_{air}) and the remainder, which represents the discrimination due to photosynthesis ($\Delta \approx \delta_{\text{leaf}} - \delta_{\text{air}}$). Upper panel, discrimination due to photosynthesis and the discrimination of purified enzyme, both relative to the WT enzyme, for the *R. rubrum* and L335V mutants. Error bars represent error propagation from δ_{leaf} S.D.

environment (δ_{air}) in each case. The air in the high CO_2 environment was more depleted in ^{13}C ($\delta_{\text{air}} \approx -18\text{‰}$) compared with the ambient air ($\delta_{\text{air}} \approx -10\text{‰}$), which accounts in part for the fact that the leaf tissue from WT tobacco grown in high CO_2 was more depleted ($\delta_{\text{leaf}} \approx -44\text{‰}$) than the leaf tissue from WT tobacco grown in ambient air ($\delta_{\text{leaf}} \approx -27\text{‰}$). The discrimination due to photosynthetic growth for each plant, this time with respect to gaseous CO_2 as the source, is given by application of Equation 4 as in Equation 15.

$$\Delta = \frac{\delta_{\text{air}} - \delta_{\text{leaf}}}{1 + \delta_{\text{leaf}}} \approx \delta_{\text{air}} - \delta_{\text{leaf}} \quad (\text{Eq. 15})$$

Hence, for WT tobacco, $\Delta \approx 17\text{‰}$ for growth in ambient air and $\Delta \approx 26\text{‰}$ for growth in 1% CO_2 . These numbers are different chiefly because discrimination is sensitive to the ratio of the

partial pressure of CO₂ at the site of carboxylation in the leaf (p_c) to the partial pressure of CO₂ in the atmosphere (p_a) according to Equation 16 (8, 48, 49),

$$\Delta \approx \bar{a} + (b - \bar{a}) \frac{p_c}{p_a} \quad (\text{Eq. 16})$$

where \bar{a} is a weighted overall fractionation due to diffusion, and b is the net discrimination due to carboxylation. At 1% CO₂, p_c/p_a will be greater than at ambient CO₂ concentrations and should approach unity. This is because when the CO₂ concentration is very large, the one-way back-leakage from the sites of carboxylation is much greater than the rate of CO₂ fixation. For two different plants (1 and 2) grown at 1% CO₂ and varying only in Rubisco, Equation 17 follows.

$$\Delta_1 - \Delta_2 \approx b_1 - b_2 \quad (\text{Eq. 17})$$

Fig. 4 also shows $\Delta - \Delta_{\text{WT}}$ for *R. rubrum* and L335V Rubiscos for both discrimination due to photosynthesis by the two mutant tobacco plants in 1% CO₂ (derived from leaf tissue) and discrimination of the purified enzymes (Δ_{Rubisco}). For the tobacco-*rubrum* plant, $\Delta_{R. rubrum} - \Delta_{\text{WT}} \approx -6\%$ for both leaf tissue and purified *R. rubrum* enzyme. For the L335V transgenic plant, $\Delta_{\text{L335V}} - \Delta_{\text{WT}} \approx -14\%$ for both leaf tissue and purified enzyme.

DISCUSSION

Δ for Purified Rubisco Can Show a Range of Values—Based on the available discrimination values for variant Rubiscos, the different enzymes can be clustered into three distinct classes according to Δ (Fig. 1). One class comprises WT tobacco Rubisco, the measured discrimination of which matches that of the other Form I Rubiscos from other higher plants, including spinach (*Spinacia oleracea*), sorghum (*Sorghum bicolor*), and soybean (*Glycine max*). A second class includes *R. rubrum* Rubisco, the measured discrimination of which matches that determined previously for this enzyme (with the possible exception of that measured by Roeske and O'Leary (50)). Within this class are included other Form II Rubiscos, such as that from a bacterial endosymbiont of the hydrothermal vent tubeworm *Riftia pachyptila*, and the cyanobacterial Form I Rubisco from *Synechococcus*, which all show comparable discrimination values. Because of its uniquely low discrimination value, L335V tobacco Rubisco constitutes a class of its own.

The two previous measurements of Δ_{Rubisco} for *R. rubrum* are notably different despite being measured under comparable experimental conditions (Table 1). Our measured value of $22.2 \pm 2.1\%$ is consistent with that of Guy *et al.* (7), who also used Rayleigh fractionation, whereas the lower Δ_{Rubisco} measured by Roeske and O'Leary (50) was determined by measuring $\delta^{13}\text{C}$ for substrate (CO₂) and product (3-phosphoglycerate) according to Equation 4.

Tcherkez *et al.* (29) demonstrated that the specificity for CO₂ over O₂ ($s_{\text{C/O}}$) and the half-saturation constant for carboxylation (K_M) are related to Δ_{Rubisco} , with lower K_M and higher $s_{\text{C/O}}$ correlated with increased Δ values. In this context, it is apparent from these results and Table 1 that Δ_{Rubisco} has been measured in a relatively restricted range of Rubiscos from autotrophic

organisms that show variation in these parameters. For example, Form ID Rubisco from red algae and non-green algae can show a wide range of K_M values, and Form IC Rubiscos from proteobacteria generally show intermediate K_M and $s_{\text{C/O}}$ values (51). In addition, there are two distinct Form IA enzymes that are either carboxysome- or non-carboxysome-associated, with the non-carboxysome form (represented by the *Solemya velum* symbiont in Table 1) having a lower K_M value (52). It has also been clearly established that the K_M of Rubisco, even within a single form, is able to adapt to the presence or absence of a CO₂-concentrating mechanism, with Rubisco from CO₂-concentrating mechanism-containing organisms having increased K_M values (51). None of this variation is represented in Table 1 or the literature, so general interpretations about how variable Δ_{Rubisco} is in nature must be tempered by the fact that not all relevant forms and variants of Rubisco have been sampled.

Δ Values for Purified Enzyme Are Consistent with Δ Values for Photosynthetic Growth—As an additional check on our measured values of discrimination for *R. rubrum* and L335V Rubiscos, we compared our values for $\Delta_{\text{Rubisco}} - \Delta_{\text{WT Rubisco}}$ for purified enzyme with those for $\Delta - \Delta_{\text{WT}}$ due to photosynthetic growth. Because genes for these enzymes were transplanted into the chloroplasts of tobacco, we are able to compare discrimination for the tobacco mutants against that for WT tobacco and neglect species-specific differences not due to Rubisco (assuming there are no pleiotropic effects, such as a change in internal conductance). For growth at high CO₂ concentration, for which the possible conductance effects become negligible, we have, from application of Equation 17, what follows in Equation 18.

$$\Delta - \Delta_{\text{WT}} \approx b - b_{\text{WT}} \quad (\text{Eq. 18})$$

The value of b represents net discrimination due to carboxylation and could include small contributions from phosphoenolpyruvate carboxylase (9, 48, 49). Even so, Fig. 4 shows that, for both *R. rubrum* and L335V Rubiscos, $\Delta_{\text{Rubisco}} - \Delta_{\text{WT Rubisco}}$ (determined from purified enzyme) does not differ significantly from $\Delta - \Delta_{\text{WT}}$ (determined from leaf tissue). Furthermore, the values do differ significantly between *R. rubrum* and L335V Rubiscos. Our discrimination values for purified enzyme are thus consistent with our discrimination values for leaf tissue where those enzymes have been transplanted into tobacco plants.

Δ Values Provide Insight into the Reaction Mechanism—Both our measurements and those of other workers (Fig. 1) show that the carbon isotope discrimination by Rubisco (Δ_{Rubisco}) is greater for higher plants than for *Synechococcus* (a cyanobacterium), *R. rubrum* (a purple, non-sulfur bacterium), and other symbiotic bacteria. As described by Tcherkez and Farquhar (20), there are two possible reasons for this: either the intrinsic isotope effect ($k_{\text{carb}}^{12}/k_{\text{carb}}^{13}$) may be lower for prokaryotic Rubiscos, reflecting a carboxylation transition state that is less product-like than for higher plants, or the carboxylated intermediate (CKABP) may be less committed to product formation in prokaryotic Rubiscos, resulting in a greater decarboxylation rate.

The first possibility is theoretically possible. Tcherkez *et al.* (29) pointed out that the more the carboxylation transition

Kinetic Isotope Effect for Three Rubiscos

state resembles its product, the shorter the O_2C-C bond of the joining CO_2 will be and thus the higher its energy and vibrational frequency. The theoretical relationship between this frequency and the kinetic isotope effect for the formation of this bond predicts that the intrinsic isotope effect ($k_{carb}^{12}/k_{carb}^{13}$) for CO_2 addition should increase as the transition state becomes more product-like. There is some support for this position from Buncel and Lee (53), who studied isotope effects resulting from the addition of OH^- during the rate-determining step in the hydrolysis of esters. Comparison of isotope effects could reveal the extent to which evolution has selected the Rubisco of a particular genotype for specificity (for CO_2 over O_2) over maximum catalytic rate (29).

There is also evidence for the second possibility. The fractionation factor for Rubisco is given by Equation 6 and has a maximum value when k_{decarb}/k_{cat} is minimized (1, 20). A lower decarboxylation rate and/or higher turnover rate would increase the specificity of Rubisco for CO_2 over O_2 if the corresponding oxygenation process, associated with photorespiration, were not similarly affected (23, 29). We know that higher plants have a lower turnover number (k_{cat}) compared with *R. rubrum* or *Synechococcus* (40, 54, 55). Therefore, it may be a lower decarboxylation rate constant that results in higher $\Delta_{Rubisco}$ for higher plants. Indeed, Pierce *et al.* (56) found that partitioning of the CKABP intermediate toward hydrolysis over decarboxylation was less (93–99%) for Rubisco derived from *R. rubrum* and *Synechococcus* than that for Rubisco from spinach (100%). For 100% partitioning toward products, $k_{decarb}/k_{cat} \approx 0$. For 95% partitioning, $k_{decarb}/k_{cat} \approx 0.05$. Thus, it is possible (for maximum discrimination during decarboxylation) that the decarboxylation rate constant (k_{decarb}) may be $\sim 5\%$ of the value of k_{cat} for prokaryotic Rubiscos. Jaworowski and Rose (57) quenched a reaction mixture of *R. rubrum* Rubisco and labeled RuBP and found that as much as 70% of the bound intermediate was returned as RuBP.

The partitioning constant for the carboxylated intermediate (p) may be defined as in Equation 19 (56).

$$p = \frac{k_{cat}}{k_{cat} + k_{decarb}} = \frac{1}{1 + k_{decarb}/k_{cat}} \quad (\text{Eq. 19})$$

The fractionation factor for Rubisco can then be expressed as in Equation 20,

$$\alpha_{Rubisco} \approx \frac{k_{carb}^{12}}{k_{carb}^{13}} \left(p + \frac{1-p}{k_{decarb}^{12}/k_{decarb}^{13}} \right) = \alpha_{carb} \left(p + \frac{1-p}{\alpha_{decarb}} \right) \quad (\text{Eq. 20})$$

where α_{carb} and α_{decarb} are the intrinsic isotope effects for carboxylation and decarboxylation, respectively. If $\Delta_{Rubisco} \approx 30\%$ represents an upper limit (equivalent to the intrinsic isotope effect (α_{cat}) for carboxylation, as suggested by Tcherkez and Farquhar (20)), then for prokaryotic Rubiscos, Equation 21 follows.

$$\alpha_{Rubisco} \approx 1.030 \left(p + \frac{1-p}{\alpha_{decarb}} \right) \quad (\text{Eq. 21})$$

Maximum intrinsic isotope effects are generally proportional to the mass difference between isotopes, which is 8% for ^{12}C and ^{13}C . Indeed, intrinsic isotope effects associated with decarboxy-

lations are generally ~ 1.065 (58). If the isotope effect for decarboxylation were near this value for prokaryotic Rubiscos and if partitioning is in the 93–99% range as found for *R. rubrum* (56), then we might expect to see discrimination reduced to 25–29% as a result of decarboxylation alone, even $<25\%$ if we account for the partitioning found by Jaworowski and Rose (57). Hence, prokaryotic Rubiscos (typified by *R. rubrum*) may exhibit less discrimination than higher plant Rubiscos (typified by WT tobacco) because they allow a greater degree of decarboxylation. This is consistent with the fact that they do not bind the carboxylated intermediate as tightly as higher plant Rubiscos, thus providing a smaller energy barrier to decarboxylation. If, however, the intrinsic isotope effect for decarboxylation is closer to the overall observed isotope effect for Rubisco-mediated carboxylation in higher plants ($\sim 30\%$), then decarboxylation alone cannot explain the lower fractionation values in *R. rubrum*.

Fig. 3 (derived from Fig. 2) shows that the enthalpic component of the free energy barrier (ΔH^\ddagger) and the associated activation energy (E_a) to the hydrolysis/cleavage step vary much more between enzymes than does the total free energy barrier (ΔG^\ddagger), which determines the rate of hydrolysis/cleavage (k_{cat}). This is because of the different contributions to free energy from the entropic components, which, in common with many solvated protein processes, results in entropy/enthalpy compensation at ambient temperatures (59).

Fig. 3 also shows the differences in entropy between the CKABP intermediate and the transition state associated with hydrolysis and cleavage ($\Delta S^\ddagger = S^\ddagger - S_{CKABP}$). Although WT tobacco undergoes a relatively small change in entropy between the enzyme-bound CKABP intermediate and the transition state, *R. rubrum* undergoes a significant decrease in entropy, whereas L335V tobacco undergoes an increase in entropy. Because the entropy change is associated with the degrees of translational and rotational freedom of the transition state (60), it might appear that Rubisco from *R. rubrum* has a more highly constrained transition state (compared with the carboxylated intermediate, CKABP) than that from WT tobacco. Rather, we suggest that the small ΔS^\ddagger value in WT tobacco Rubisco is consistent with the assumption of a tightly bound CKABP intermediate. Thus, the binding constant of the latter is closer to that of a transition state rather than a substrate. As a result, there is no important difference in the number of degrees of freedom between WT tobacco CKABP and the transition state for hydrolysis/cleavage. By contrast, in the *R. rubrum* enzyme, the CKABP molecule is much less tightly bound, and there is a large difference in the degrees of freedom between CKABP and the transition state. In addition, because *R. rubrum* Rubisco has a significantly lower activation energy compared with WT tobacco, it results overall in a lower total free energy change for hydrolysis/cleavage (and hence a faster k_{cat}).

On the other hand, L335V tobacco Rubisco has a higher activation energy compared with WT tobacco Rubisco and a higher total free energy change (and hence a slower k_{cat}). We also note that the entropic component associated with hydration/cleavage is positive; this indicates that the restriction of the degrees of freedom is very weak at the transition state level compared with the CKABP molecule, which is tightly bound (see above).

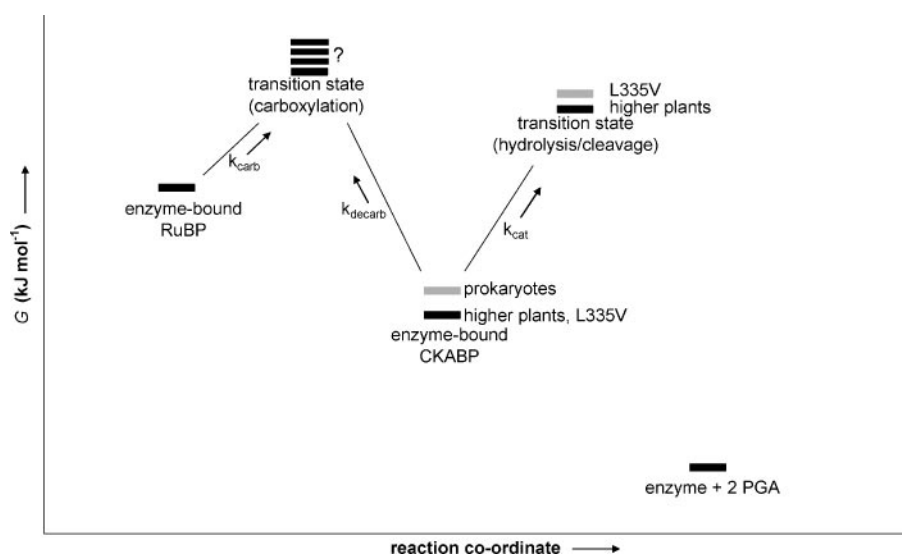


FIGURE 5. Proposed free energy landscape for the carboxylation, decarboxylation, and hydrolysis/cleavage steps of Form I Rubisco from higher plants, prokaryotic Rubisco, and L335V mutant tobacco Rubisco. PGA, 3-phosphoglycerate.

In other words, this would agree with a very “loose” transition state for hydrolysis/cleavage in the L335V enzyme. This is then accompanied by a loss of catalytic efficiency, as revealed by the slower rate and the higher activation energy than compared with WT tobacco (Fig. 3).

It appears likely then that the L335V mutant Rubisco exhibits a lower fractionation because of its crippled hydrolysis/cleavage rate, which would result in a higher energy barrier for hydrolysis/cleavage and a greater degree of decarboxylation. The discrimination value of the L335V enzyme may be explained by a partitioning factor of ~ 0.7 and a decarboxylation fractionation factor of 1.065. Such parameter values result from a k_{cat} that is ~ 10 times less than that of WT Rubisco, consistent with our measured k_{cat} values (Fig. 2). In other words, the commitment of the carboxylated intermediate to hydrolysis/cleavage is diminished, even though this intermediate is bound just as tightly by L335V Rubisco as it is by WT tobacco Rubisco (61). Given the relationship between the transition state and the fractionation as argued by Tcherkez *et al.* (29), it is unlikely then that L335V tobacco Rubisco has a lower intrinsic isotope effect associated with the CO_2 addition step (and hence a less product-like transition state for this step). The case of the L335V mutant tobacco differs fundamentally from prokaryotic and higher plant Rubiscos, as it is unlikely to be on the locus of evolutionary optimization. However, it suggests that decarboxylation of enolized RuBP is physically possible.

The two explanations for differences in fractionation between Rubiscos are thus not mutually exclusive: both a more product-like transition state associated with carboxylation (which may cause a stabilization of the CKABP intermediate) and a reduction in the rate of decarboxylation may cause increases in the carbon isotope fractionation of higher plants. The impact of decarboxylation will be appreciable only if the intrinsic isotope effect for decarboxylation (α_{decarb}) is significantly greater than that for carboxylation. It is likely then that the major origin of the larger $^{12}\text{C}/^{13}\text{C}$ discrimination of the higher plant enzyme is a more

advanced transition state for carboxylation. On the other hand, the L335V mutant has a lower fractionation mainly because of the enhancement of decarboxylation.

Fig. 5 shows a proposed energy landscape for carboxylation, decarboxylation, and hydrolysis/cleavage for the three enzymes (as representatives of the three Δ classes). The energy of the carboxylation transition state for any of the enzymes is indeterminate in Fig. 5, as we cannot measure it. The relative energy of the enzyme-bound CKABP intermediate for prokaryotic Rubisco is greater than that for higher plant Rubiscos. In contrast to *R. rubrum*, L335V mutant tobacco Rubisco appears to bind 2-carboxy-D-arabinitol 1,5-bisphosphate as tightly

as WT tobacco Rubisco (61).

Although *R. rubrum* Rubisco has a higher k_{cat} than does WT tobacco Rubisco, it may not be enough to prevent an increase in decarboxylation over the WT enzyme, possibly reflected in a higher energy hydrolysis/cleavage transition state than that for WT enzyme. The L335V mutation in tobacco results in a higher free energy for the transition state, but with a decrease, rather than an increase, in k_{cat} (due to its CKABP intermediate being more tightly bound than in prokaryotes). Thus, L335V may suffer the double inefficiency of a reduced k_{cat} and increased decarboxylation. Its Δ value is even less than that for *R. rubrum*.

Under the selective pressure of low $[\text{CO}_2]$, high $[\text{O}_2]$ terrestrial environments, Rubiscos from higher plants with the C_3 photosynthetic pathway appear to have eliminated the decarboxylation reaction, which may exist for enzymes of prokaryotes of high $[\text{CO}_2]$, low $[\text{O}_2]$ environments. Such an evolutionary trend probably proceeded by modifying the carboxylation transition state toward a more advanced geometry as a response to the need to reduce the oxygenation reaction (29). Efforts to artificially improve Rubisco for higher plants may therefore be restricted by the trade-off between increasing the turnover number (k_{cat}) on the one hand and elevating the enzyme specificity ($s_{\text{C/O}}$) and affinity (lower K_M) for CO_2 on the other. Thus, the potential for genetically modifying the enzyme may necessitate the manipulation of residues that have an impact on the carboxylation and hydrolysis/cleavage transition states. It should be possible to address these hypotheses and to identify mechanisms underlying the natural kinetic variability of Rubiscos by further screening the carbon isotope discrimination and the temperature dependences of k_{cat} and $s_{\text{C/O}}$ for isolated Rubisco from a broader range of photosynthetic organisms.

Acknowledgments—We thank Hilary Stuart-Williams and Sue Wood for carbon isotope analysis of air and leaf samples and Chin Wong for help with CO_2 trapping from air.

REFERENCES

- Paneth, P., and O'Leary, M. H. (1985) *Biochemistry* **24**, 5143–5147
- Whelan, T., Sackett, W. M., and Benedict, C. R. (1973) *Plant Physiol.* **51**, 1051–1054
- Reibach, P. H., and Benedict, C. R. (1977) *Plant Physiol.* **59**, 564–568
- O'Leary, M. H., Rife, J. E., and Slater, J. D. (1981) *Biochemistry* **20**, 7308–7314
- Christeller, J. T., Laing, W. A., and Troughton, J. H. (1976) *Plant Physiol.* **57**, 580–582
- Roeske, C. A., and O'Leary, M. H. (1984) *Biochemistry* **23**, 6275–6284
- Guy, R. D., Fogel, M. L., and Berry, J. A. (1993) *Plant Physiol.* **101**, 37–47
- Farquhar, G. D., O'Leary, M. H., and Berry, J. A. (1982) *Aust. J. Plant Physiol.* **9**, 121–137
- Farquhar, G. D., and Richards, R. A. (1984) *Aust. J. Plant Physiol.* **11**, 539–552
- Farquhar, G. D. (1983) *Aust. J. Plant Physiol.* **10**, 205–226
- von Caemmerer, S. (1989) *Planta* **178**, 463–474
- Griffiths, H., Broadmeadow, M. S. J., Borland, A. M., and Hetherington, C. S. (1990) *Planta* **181**, 604–610
- Griffiths, H. (1992) *Plant Cell Environ.* **15**, 1051–1062
- Griffiths, H., Cousins, A. B., Badger, M. R., and von Caemmerer, S. (2007) *Plant Physiol.* **143**, 1055–1067
- O'Leary, M. H. (1981) *Phytochemistry* **20**, 553–567
- O'Leary, M. H., Madhavan, S., and Paneth, P. (1992) *Plant Cell Environ.* **15**, 1099–1104
- Craig, H. (1957) *Geochim. Cosmochim. Acta* **12**, 133–149
- Kroopnick, P., and Craig, H. (1976) *Earth Planet. Sci. Lett.* **32**, 375–388
- Lane, G. A., and Dole, M. (1956) *Science* **123**, 574–576
- Tcherkez, G., and Farquhar, G. D. (2005) *Funct. Plant Biol.* **32**, 277–291
- Laing, W. A., and Christeller, J. T. (1976) *Biochem. J.* **159**, 563–570
- Badger, M. R., and Collatz, G. J. (1977) *Carnegie Inst. Wash. Year Book* **76**, 355–361
- Andrews, T. J., and Lorimer, G. H. (1987) in *The Biochemistry of Plants: A Comprehensive Treatise* (Hatch, M. D., and Boardman, N. K., eds) Vol. 10, pp. 131–218, Academic Press, New York
- Schloss, J. V., and Lorimer, G. H. (1982) *J. Biol. Chem.* **257**, 4691–4694
- Lorimer, G. H., Andrews, T. J., Pierce, J., and Schloss, J. V. (1986) *Philos. Trans. R. Soc. Lond. B Biol. Sci.* **313**, 397–407
- Berti, P. J. (1999) in *Enzyme Kinetics and Mechanism. Part E: Energetics of Enzyme Catalysis* (Schramm, V. L., and Purich, D. L., eds) pp. 355–397, Academic Press, San Diego, CA
- Bigeleisen, J. (1949) *J. Chem. Phys.* **17**, 675–678
- Melander, L. C. S. (1960) *Isotope Effects on Reaction Rates*, Ronald Press, New York
- Tcherkez, G. G. B., Farquhar, G. D., and Andrews, T. J. (2006) *Proc. Natl. Acad. Sci. U. S. A.* **103**, 7246–7251
- Spreitzer, R. J. (1999) *Photosynth. Res.* **60**, 29–42
- Andersson, I., and Taylor, T. C. (2003) *Arch. Biochem. Biophys.* **414**, 130–140
- Whitney, S. M., von Caemmerer, S., Hudson, G. S., and Andrews, T. J. (1999) *Plant Physiol.* **121**, 579–588
- Gutteridge, S., and Gatenby, A. A. (1995) *Plant Cell* **7**, 809–819
- Taylor, T. C., and Andersson, I. (1996) *Nat. Struct. Biol.* **3**, 95–101
- McNevin, D., Badger, M. R., Kane, H. J., and Farquhar, G. D. (2006) *Funct. Plant Biol.* **33**, 1115–1128
- Whitney, S. M., and Andrews, T. J. (2001) *Proc. Natl. Acad. Sci. U. S. A.* **98**, 14738–14743
- Kane, H. J., Wilkin, J. M., Portis, A. R., and Andrews, T. J. (1998) *Plant Physiol.* **117**, 1059–1069
- Servaites, J. C. (1985) *Arch. Biochem. Biophys.* **238**, 154–160
- Edmondson, D. L., Badger, M. R., and Andrews, T. J. (1990) *Plant Physiol.* **93**, 1376–1382
- Morell, M. K., Kane, H. J., and Andrews, T. J. (1990) *FEBS Lett.* **265**, 41–45
- Andrews, T. J., and Kane, H. J. (1991) *J. Biol. Chem.* **266**, 9447–9452
- Butz, N. D., and Sharkey, T. D. (1989) *Plant Physiol.* **89**, 735–739
- Ruuska, S., Andrews, T. J., Badger, M. R., Hudson, G. S., Laisk, A., Price, G. D., and von Caemmerer, S. (1998) *Aust. J. Plant Physiol.* **25**, 859–870
- Pierce, J., Tolbert, N. E., and Barker, R. (1980) *Biochemistry* **19**, 934–942
- Mook, W. G., Bommerson, J. C., and Staverman, W. H. (1974) *Earth Planet. Sci. Lett.* **22**, 169–176
- Andrews, T. J. (1988) *J. Biol. Chem.* **263**, 12213–12219
- Wright, G. C., Hubick, K. T., and Farquhar, G. D. (1988) *Aust. J. Plant Physiol.* **15**, 815–825
- Farquhar, G. D., Ehleringer, J. R., and Hubick, K. T. (1989) *Annu. Rev. Plant Physiol.* **40**, 503–537
- Brugnoli, E., and Farquhar, G. D. (2000) in *Photosynthesis: Physiology and Metabolism* (Leegood, R. C., Sharkey, T. D., and von Caemmerer, S., eds) pp. 399–434, Kluwer Academic Publishers, Norwell, MA
- Roeske, C. A., and O'Leary, M. H. (1985) *Biochemistry* **24**, 1603–1607
- Badger, M. R., Andrews, T. J., Whitney, S. M., Ludwig, M., Yellowlees, D. C., Leggat, W., and Price, G. D. (1998) *Can. J. Bot.* **76**, 1052–1071
- Badger, M. R., and Bek, E. J. (2008) *J. Exp. Bot.*, in press
- Buncel, E., and Lee, C. C. (1977) *Carbon-13 in Organic Chemistry*, Elsevier Science Publishing Co., Inc., New York
- Andrews, T. J., and Lorimer, G. H. (1985) *J. Biol. Chem.* **260**, 4632–4636
- Morell, M. K., Paul, K., Oshea, N. J., Kane, H. J., and Andrews, T. J. (1994) *J. Biol. Chem.* **269**, 8091–8098
- Pierce, J., Andrews, T. J., and Lorimer, G. H. (1986) *J. Biol. Chem.* **261**, 248–256
- Jaworowski, A., and Rose, I. A. (1985) *J. Biol. Chem.* **260**, 944–948
- O'Leary, M. H. (1988) *Acc. Chem. Res.* **21**, 450–455
- Cooper, A. (1999) *Curr. Opin. Chem. Biol.* **3**, 557–563
- Moore, W. J. (1983) *Basic Physical Chemistry*, Prentice-Hall International, London
- Pearce, F. G., and Andrews, T. J. (2003) *J. Biol. Chem.* **278**, 32526–32536
- Scott, K. M., Schwedock, J., Schrag, D. P., and Cavanaugh, C. M. (2004) *Environ. Microbiol.* **6**, 1210–1219
- Wong, W. W., Benedict, C. R., and Kohel, R. J. (1979) *Plant Physiol.* **63**, 852–856
- Robinson, J. J., Scott, K. M., Swanson, S. T., O'Leary, M. H., Horken, K., Tabita, F. R., and Cavanaugh, C. M. (2003) *Limnol. Oceanogr.* **48**, 48–54
- Farquhar, G. D. (1979) *Arch. Biochem. Biophys.* **193**, 456–468
- von Caemmerer, S. (2000) *Biochemical Models of Leaf Photosynthesis*, CSIRO Publishing, Collingwood, Victoria, Australia